Science of the Total Environment 756 (2021) 143805

Contents lists available at ScienceDirect

Science of the Total Environment

journal homepage: www.elsevier.com/locate/scitotenv

Study of the photoinduced transformations of sertraline in aqueous media

Paola Calza [a], Cristina Jiménez-Holgado [b], Marco Coha [a], Christoforos Chrimatopoulos [b], Federica Dal Bello [c], Claudio Medana [c], Vasilios Sakkas [b,*]

[a] Department of Chemistry, Via Giuria 5, 10125, Università degli Studi di Torino, Torino, Italy
[b] Department of Chemistry, University of Ioannina, Laboratory of Analytical Chemistry, Ioannina 45 110, Greece
[c] Department of Molecular Biotechnology and Health Sciences, Via Giuria 5, 10125 Torino, Italy

HIGHLIGHTS

- $T_{1/2}$ of sertraline decreased from 57 h in ultrapure water to 7 h in aqueous solution of 10 mg/L HA.
- Sertraline showed high degradation rate in photocatalysis with TiO_2.
- Forty-four transformation products were identified.
- More toxic compounds were produced in the first stages of photocatalysis.

GRAPHICAL ABSTRACT

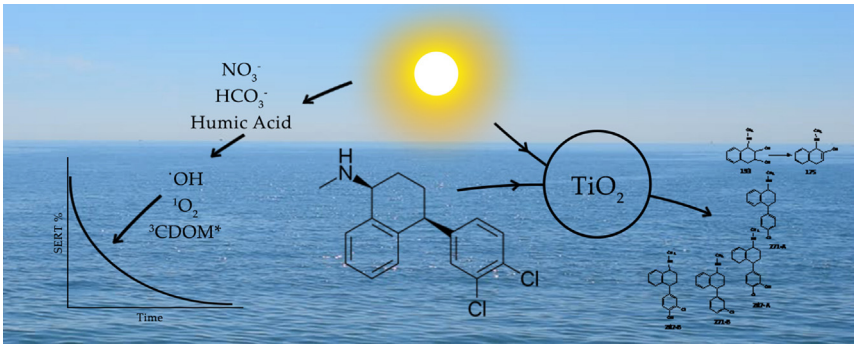

ARTICLE INFO

Article history:
Received 15 July 2020
Received in revised form 25 October 2020
Accepted 25 October 2020
Available online 27 November 2020

Editor: Dimitra A Lambropoulou

Keywords:
Antidepressants
Photodegradation
Photosensitizers
Photocatalysis
Toxicity
Transformation products

ABSTRACT

In the present study, the photoinduced degradation of the antidepressant drug sertraline under artificial solar radiation was examined. Photolysis was studied under different experimental conditions to explore its photolytic fate in the aqueous environment. Photolytic degradation kinetics were carried out in ultrapure water, wastewater effluent, as well as in the presence of dissolved organic matter (humic acids), bicarbonate and nitrate ions which enabled their assessment on sertraline photo-transformation. The reaction of sertraline with photoactive compounds accelerated sertraline transformation in comparison with direct photolysis. Moreover, TiO_2-mediated photocatalytic degradation of sertraline was investigated, and focus was placed on the identification of by-products. As expected, photocatalysis was extremely effective for sertraline degradation. Photocatalytic degradation proceeded through the formation of forty-four transformation products identified by HPLC-HRMS and after 240 min of irradiation total mineralization was achieved. Microtox bioassay (*Vibrio fischeri*) was employed to assess the ecotoxicity of the photocatalysis-treated solutions and results have indicated that sertraline photo-transformation proceeds through the formation of toxic compounds.

1. Introduction

Antidepressants are medications that can help relieve symptoms of depression, social anxiety disorder, anxiety disorders, seasonal affective disorder, and dysthymia, or mild chronic depression, as well as other conditions. As with other emerging pollutants, these compounds enter

* Corresponding author at: Department of Chemistry, University of Ioannina, Panepistimioupolis, 45110 Ioannina, Greece.
E-mail address: vsakkas@uoi.gr (V. Sakkas).

https://doi.org/10.1016/j.scitotenv.2020.143805

the aquatic environment mainly through effluents from wastewater treatment plants (WWTPs) and hospitals (Hernando et al., 2006). The presence and fate of these chemicals in wastewater and receiving waters has attracted the attention from the scientific community.

There is a growing public and scientific concern about the effects on ecosystem and human health posed by the presence of pharmaceuticals in the environment. Over the last few decades, the fate and occurrence and effects of pharmaceutical compounds, including psychiatric drugs, in the aquatic environment (*i.e.* drinking water, groundwater, surface water and treated water) was assessed (Kosjek and Heath, 2010; Hörsing et al., 2012; Ofoegbu et al., 2019; Kosjek et al., 2005; Xiang et al., 2018; Wu et al., 2015; Baker and Kasprzyk-Hordern, 2011). Psychiatric drugs in surface water and wastewater have been reported in a wide range of concentration levels from ppt to several ppb over the world (Xiang et al., 2018; Wu et al., 2015; Baker and Kasprzyk-Hordern, 2011).

Once released in the surface water, they can be subjected to several attenuation processes such as hydrolysis, biodegradation, adsorption and photolysis (Kosjek and Heath, 2008; Nassar et al., 2017). Photochemical reactions occurring in surface waters, that comprises direct and indirect photolysis, play a key role in their environmental attenuation. In the case of direct photolysis, sunlight absorption by the pollutant triggers its transformation (Katagi, 2018). As far as indirect photochemistry is concerned, sunlight is absorbed by photoactive compounds called photosensitizes (Pozdnyakov et al., 2020). Upon sunlight absorption, these compounds produce reactive transients such as the hydroxyl radical (•OH), singlet oxygen ($^1O_2$) and CDOM triplet states (^{3}CDOM*), which can induce pollutant transformation (Vione et al., 2014). Natural water constituents such as nitrates, bicarbonate and especially dissolved organic matter play an important role in the photolytic degradation of organic compounds since they can participate in the production of the above-mentioned reactive species (Kang et al., 2018). Therefore, indirect photolysis has been found as an environmentally important elimination way of organic pollutants, including pharmaceutical compounds and personal care products. Accordingly, identifying their effect on sertraline photo-transformation was of interest.

Sertraline occurrence in wastewater and surface waters has been reported at concentration levels from 2 ng/L up to few μg/L (Mole and Brooks, 2019; Xie and Lu, 2019; Gornik et al., 2020).

Low to moderate removal rates (25–48%) of sertraline from WWTPs (Lajeunesse et al., 2012) implicates search for alternative and more effective methods. The exploitation of Advanced Oxidation Processes is among the possible ways for increasing the treatment efficiency. In particular, the use of photocatalysis could be a powerful solution for environmental remediation, and TiO_2 is among the most commonly used and effective metal oxides (Talwar et al., 2018; El Mouchtari et al., 2020).

Considering the fact that sertraline residues have been detected in environmental aquatic systems, firstly the aim of this work was to perform experiments under simulated solar radiation in ultrapure water as a reference (without matrix components) and in an effluent of WWTP to investigate its photolytic fate; to simulate a natural process that occurs in the environment. The effects of natural organic matter, nitrate and bicarbonate ions were also studied. Moreover, AOPs were applied for the abatement of pollution caused by the presence of residual sertraline in waters. Special attention has been given to the assessment of the photocatalytic transformation of sertraline, using mild experimental conditions to identify possible transformation byproducts evolved and suggest possible degradation pathways. Finally, toxicity assessment was followed based on the bioluminescent bacterium, Vibrio fischeri and US EPA ECOSAR computer model.

2. Experimental details

2.1. Reagents

Antidepressant sertraline (SERT) was purchased from TCI Tokyo Chemical Industry (Tokyo, Japan). The analyte has purity higher than 98%. For analytical purposes sertraline was dissolved in methanol to provide a stock solution containing 1000 mg/L of analyte. The solution was stored in glass-stopped bottles at −20 °C in the dark. Standard working solutions were prepared, daily. Ultrapure water used was produced by a Milli-Q system (Evoqua, Pittsburg, USA). Photosensitizers: humic acid, $NaNO_3$ and $NaHCO_3$ were purchased from Sigma-Aldrich (Athens, Greece). Irradiation procedures of sertraline were carried out by experimental solutions that were prepared by dissolving sertraline directly in ultrapure water, ultrapure water+sensitizers, WWTP effluent. The latter was collected from the WWTP of the city of Ioannina in amber glass bottles pre-rinsed with deionized water. Up on their arrival in the laboratory, were centrifuged (4000 rpm, 25 °C, 10 min) and filtered with 0.2-μm polypropylene (PP) filters to eliminate the particulate matter. Wastewater characterization parameters are given at Table S1.

2.2. Irradiation procedures

2.2.1. Direct and indirect photolysis

Aqueous solutions of sertraline (1 mg/L, 50 mL) were irradiated under simulated solar conditions using a Suntest CPS+ apparatus from Heraeus (Hanau, Germany) equipped with a Xenon arc lamp (1500 W). The runs were performed adjusting the lamp power to 750 W m^{-2} with a simulated solar emission within 300 to 800 nm. The lamp was equipped with a glass filter that inhibits the transmission of wavelengths under 290 nm. Solutions were irradiated in a 100 mL Pyrex glass UV-reactor with a flat flange lid with three necks. Samples were irradiated under magnetic stirring. A tap-water cooling system was used, for samples to not exceed 25 °C. Aliquots (0.5 mL) were withdrawn from the photoreactor at specific time intervals.

In order to examine the effect of humic acids (2.5, 5.0, 10 mg/L), nitrate (2.5, 5.0, 10 mg/L) and bicarbonate ions (2.5, 5.0, 10 mg/L), aqueous sertraline solutions (1 mg/L) in ultrapure water (50 mL), were exposed to artificial solar light (Suntest).

The kinetics of reaction is analyzed directly from the concentration *versus* time curves. The first-order equation $C_t = C_o\, e^{-kt}$: was applied to determine the rate constant (C_t is sertraline concentration at time t, C_o is the initial concentration and k is the rate constant).

2.2.2. Photocatalytic procedures

Sertraline photocatalytic degradation in ultrapure water was carried out in Pyrex glass cells (2.3 cm height × 4.0 cm diameter), filled with 5 mL of sertraline (20 mg/ L) and TiO_2 (400 mg/ L) suspension kept under magnetic stirring. Samples were irradiated for different times using a PHILIPS Cleo 6 × 15 W TL-D Actinic BL with maximum emission wavelength at 365 nm. The UV integrated irradiance on the cells in the 290–400 nm range wavelengths was 90 ± 2 Wm^{-2} (measured with a CO.FO.MEGRA. (Milan, Italy) power-meter). After irradiation, samples were filtered through a 0.45 μm filter and analyzed with the proper analytical technique. In all studied photoinduced processes, the decomposition rate of sertraline fitted a pseudo-first kinetics model.

2.3. Analytical procedures

Kinetics from direct and indirect photolysis were followed by a Thermo Scientific UltiMate 3000 HPLC system equipped with a diode array detector and Chromeleon Thermo Scientific software. The equipment consists of a Binary Solvent Manager (BSM), a WPS-3000SL autosampler and a column manager all from Waters Thermo Scientific (Waltham, Massachusetts, USA). The injection volume into the chromatographic equipment was 20 μL, and the analytical column was a Hypersil GOLD 150 × 4.6 mm, with a particle size of 5 μm (Thermo Scientific, Waltham, Massachusetts, USA) operating at 25 °C. The mobile phase consists of methanol (A) and water with 0.3% phosphoric acid (B), at 1.0 mL/min flow in gradient mode. The gradient starts at 15:85 (A:B) (v/v) and is increasing in 3 min to 50% methanol. The percentage of methanol further increased up to 80% in 7 min and the gradient

returned in 2 min to the first state 15:85 (equilibrium time 3 min). The whole chromatographic separation process finished in 15 min. The UV detector was set at 245 nm.

The degradation of sertraline and the identification of its transformation products (TPs) in ultrapure water was followed using an Ultimate 3000 High Pressure Liquid Chromatography coupled through an ESI source to an LTQ-orbitrap mass spectrometer (Thermo Scientific, Bremen, Germany). The chromatographic separation was achieved with a reverse phase C18 column (Gemini NX C18, 150 × 2 mm, 3 μm, 110 Å; Phenomenex, Castel Maggiore, BO, Italy) using 5 mM aqueous heptafluorobutanoic acid (eluent A) and acetonitrile (eluent B). Gradient separation ramp started with 5% B, increased up to 40% B in 18 min and to 100% in 5 min; then the column came back to the initial conditions.

The LC mobile phase was delivered to ESI ion source using nitrogen both as sheath and auxiliary gas. Source parameters were set as followed: sheath gas 30 arbitrary unit (arb), auxiliary gas 25 arb, capillary voltage 4.0 kV and capillary temperature 275 °C. Full mass spectra were acquired in positive ion mode in the *m/z* range between 50 and 500, with a resolution of 30 k. MS^n spectra were acquired in the range between ion trap cut-off and precursor ion *m/z* values. Precursor ions were focused in a window of 3 Da width, for supposed chlorinated species the width was extended to 5 Da. Mass accuracy of recorded ions (*versus* calculated) was ±0.001 u (without internal calibration).

As described by Zhu et al. (2006) the photocatalysis degradation processes that characterize the photodegradation operation brought to a customized list of the main unknown *m/z* values of the hypothetic transformation products derived from sertraline. The customized list of suspected TPs was prepared using Xcalibur software (Xcalibur 4.1). In particular we searched for the following "known-unknowns" derivatives: mono-hydroxylated (322 *m/z*), di-hydroxylated (338 *m/z*), tri-hydroxylated (354 *m/z*), oxidized (304 *m/z*), oxidized/mono-hydroxylated (320 *m/z*), oxidized/di-hydroxylated (336 *m/z*), oxidized/tri-hydroxylated (352 *m/z*), dechlorinated (272 *m/z*), dechlorinated/mono-hydroxylated (288 *m/z*). By Xcalibur software additional non target analytes were identified after manual inspection of the chromatograms ("unknown unknowns" based on signal/noise value). Three technical replicates for each time point was performed. Isotope ratio was manually checked in the case of supposed chlorinated species, using isotopic pattern simulator of Xcalibur software. M + 2 and M + 4 ion intensity of the hypothesized molecules was confirmed within ±10% of relative values.

Total organic carbon (TOC) was measured using a Shimadzu TOC-5000 analyzer (catalytic oxidation on Pt at 680 °C). The calibration was performed using standards of potassium phthalate.

Inorganic ions formed during sertraline degradation were identified by ion chromatography analysis using a Dionex chromatograph equipped with a Dionex 40 ED pump and Dionex 40 ED conductimetric detector. For chloride, nitrate and nitrite anions, a Dionex Ion Pac AS9-HC 4 × 250 mm column, and Ion Pac ASRS-ULTRA 4 mm conductivity suppressor was applied. Ammonium was analyzed using a Dionex Ion Pac CS12A 4 × 250 mm column, and Ion Pac CSRS-ULTRA 4 mm conductivity suppressor, using 9 mM Na_2CO_3 as eluent at 1 mL/min.

2.4. Toxicity

The acute toxicity of sertraline and its transformation products in ultrapure water in the presence of TiO_2 (400 mg/ L) was evaluated using a Microtox Model 500 toxicity analyzer (Milan, Italy). The analysis was performed evaluating the bioluminescence inhibition assay in the marine bacterium *Vibrio fischeri* by monitoring changes in the natural emission of the luminescent bacteria. Freeze-dried bacteria, reconstitution solution, diluent (2% NaCl) and an adjustment solution (non-toxic 22% sodium chloride) were obtained from Azur (Milan, Italy). Samples were tested in a medium containing 2% sodium chloride, and the luminescence was recorded after 5, 15 and 30 min of incubation at 15 °C. The luminescence inhibition percentage was determined by comparing with a non-toxic control. Moreover, the acute toxicity of SER and its transformation products to three aquatic organisms was assessed employing the ECOSAR model v2.0. The chronic toxicity concentrations for these organisms were also calculated using ECOSAR (Tay and Madehi, 2015; Kuang et al., 2013).

3. Results and discussion

3.1. Photolytic degradation

Direct photolysis of sertraline in ultrapure water and in WWTP effluent under artificial solar irradiation, followed a first order kinetics (Fig. 1). Sertraline photolysis at the effluent of WWTP is greater than ultrapure water showing a strong dependence on the constitution of the irradiated media. To be more specific, when sertraline was irradiated in ultrapure water, a half-life ($t_{1/2}$) of 57 h was found. However, when sertraline was irradiated at different aqueous matrix (effluent of WWTP) the rate constant increased almost 40%, ($t_{1/2}$ decreased to 34 h, Table 1). There are several parameters that may affect the photodegradation process: radiation source, presence of organic and inorganic substances, pH *etc.* Jakimska et al. (n.d.) have conducted photolytic degradation experiments of sertraline at the same concentration level (1 mg/L) in a variety of experimental conditions employing natural solar irradiation as well as xenon lamp. Pseudo-first order degradation kinetics were followed, and sertraline photolysis was faster in natural waters in comparison to ultrapure water attributed to autocatalytic reactions (Jakimska A et al., n.d.). However, there were no solid conclusions with regards to the effects of different water matrices. It is well documented in the literature that natural water constituents such as dissolved organic matter, nitrates, and bicarbonates are significant participants in the photochemical degradation of organic microcontaminants in surface waters. Studies have shown that DOM can promote or inhibit the photolysis of organic pollutants (Vione et al., 2014). The promotion mechanism is mainly through indirect photolysis processes such as photosensitized oxidation reaction. This behavior has been reported also for other antidepressants such as clozapine (Trawiński and Skibiński, 2019). Inhibition mechanism is mainly embodied in the abundant conjugated chromophore structure in DOM, which may be related to the photo-shielding effect of organic pollutants competing to absorb light and the quenching effect of DOM on the excited state of pollutants. In addition, the presence of bicarbonate or nitrate ions hastens the photoinduced reactions thanks to the production of reactive oxygen species (ROS) (Kang et al., 2018). Therefore, in our study to investigate their reactivity on the photodegradation of sertraline, experiments were carried out in ultrapure water and different environmentally realistic concentrations of humic acids, nitrate, and bicarbonate ions.

Fig. 1 depicts the degradation curves of the antidepressant in different irradiation conditions specified at Table 1. Our data clearly demonstrate that humic acids (HA) greatly increase the rate of sertraline photo-transformation ($t_{1/2}$ = 7 *h*, when HA = 10 mg/L). HA can promote sertraline photolysis, by acting as a photosensitizer through the generation of •OH and O_2 (Niu et al., 2013; Trawiński and Skibiński, 2017), suggesting that natural organic matter (NOM) would affect the photolytic process, particularly at high concentrations. Recently, Gornik et al. (2019), investigated the photo-transformation of sertraline (at 0.01 and 1 mg/L, 125 W medium pressure mercury lamp) under laboratory scale measurements in different matrices chosen based on the requirements of the modelling software APEX (Aqueous Photochemistry of Environmentally-occurring Xenobiotics). Results have shown that photodegradation is pH dependent, resulting in fastest degradation at the alkaline pH, as observed in our study (ultrapure water *vs* WWT effluent). Moreover, in agreement with our findings, the presence of photosensitizers such as dissolved organic matter, nitrate and carbonate/

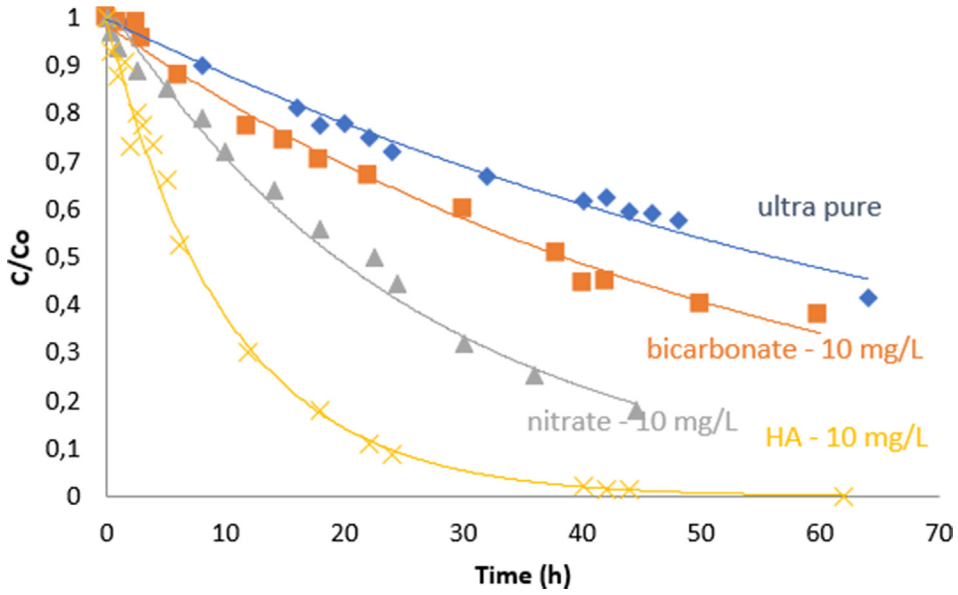

Fig. 1. Kinetics of sertraline in direct and indirect photolysis.

bicarbonate ions accelerated the photolysis reaction rate in comparison to ultrapure water (Gornik et al., 2019).

The degradation rates in the presence of OH radicals produced by nitrate photolysis, was higher compared to ultrapure water (Table 1). Increased concentrations of NO_3^- from 2.5 to 10 mg/L have a positive effect on the photodegradation rate, with $t_{1/2}$ comprising between 35 and 18 h. Considering the effect of carbonate radicals that were produced in the presence of different bicarbonate concentrations (2.5–10 mg/L, and 1 mg/L of nitrate), results have demonstrated that carbonate radicals enhance the degradation of sertraline although to a much lesser extent compared to organic matter and nitrate. Even if studies have shown that sertraline is affected by irradiation, and undergoes direct/indirect degradation, it does not mean that the contamination problem is solved since photo-transformation products formed can be more toxic than the parent molecules (Trawiński and Skibiński, 2017). The effectiveness of the photodegradation efficiency could be dramatically increased by employing AOPs (Minero et al., 1999; Sugihara et al., 2013; Calza et al., 2006; Klavarioti et al., 2009).

3.2. Photocatalytic performance

The introduction of the TiO_2 as photocatalyst (Minero et al., 1999; Sugihara et al., 2013; Calza et al., 2006) strongly enhanced the process,

Table 1
Degradation kinetic parameters of sertraline in different aqueous media under artificial solar irradiation.

		R^2	k (h^{-1})	$t_{1/2}$ (h)
Ultrapure water		0.9767	0.012	58
WWTP		0.9968	0.0203	34
HA	2.5	0.9889	0.0193	36
(mg/L)	5	0.9855	0.0313	22
	10	0.9984	0.0978	7
$NaNO_3$ (mg/L)	2.5	0.9762	0.0198	35
	5	0.9907	0.0242	29
	10	0.9823	0.0380	18
$NaHCO_3$[a] (mg/L)	2.5	0.9867	0.0126	55
	5	0.9735	0.0141	49
	10	0.9850	0.0180	39

[a] Nitrate 1 mg/L was present to assist on $CO_3^{\bullet -}$ production.

and after 1 h of irradiation, both parent molecule and its TPs were mineralized.

As regards the mineralization process, after only 1 h of irradiation, the TOC was <5% of the initial organic carbon (Fig. 2). Chlorine atoms are released faster than nitrogen and they reach the stoichiometric amount within 1 h of irradiation. Nitrogen is mainly released as ammonium (Sugihara et al., 2013; Calza et al., 2006) and it reaches the stoichiometric amount after 1 h of irradiation, when ammonium accounts for almost 75% and nitrate 25% of the stoichiometric amount. Although pharmaceuticals found in the outlet of municipal WWTPs may not require immediate attention regarding their removal, treatment-at-source may still be a plausible option replacing conventional chlorination by an AOP induced disinfection/oxidation technique (Klavarioti et al., 2009). Our findings suggest that consideration of advanced treatment strategies like photocatalysis may overcome the limitations of primary and secondary treatment processes to eliminate sertraline residues in wastewater. Moreover, the attention should also be given to the potential that removal of these drugs following AOPs could lead to the evolution of by-products that would need to be identified, quantified and evaluated for their biological activity (Lajeunesse et al., 2012). For this reason, all samples were analyzed *via* HPLC coupled with high-resolution mass spectrometry (Orbitrap) with an electrospray ionization source in positive ion mode for the identification of sertraline transformation products. The photocatalytic process used for the abatement of sertraline leads to the formation of forty-four transformation products, as can be observed all of them are completely abated in 40–60 min. Fig. 3 depicts a representative LC-HRMS chromatogram showing main TPs formation at 5 min of photocatalytic degradation.

3.3. Structural elucidation of the transformation products

The accurate mass for all transformation products (TP) was established, so allowing to obtain their empirical formulae and are collected in Table 2. MS^2 and MS^3 spectra analysis permits to assign a tentative structure for most of the transformation products; all MS^n fragments are reported in Tables S2-S10 as Supplementary Information, while MS^2 spectra and the proposed fragmentation pathways are shown in Figs. S1–S23.

A level of confidence recommended by Schymanski et al. (2014) was assigned to each TP and is reported in Table 2 as well. Aiming at TPs structural elucidation, the sertraline fragmentation pathway was firstly

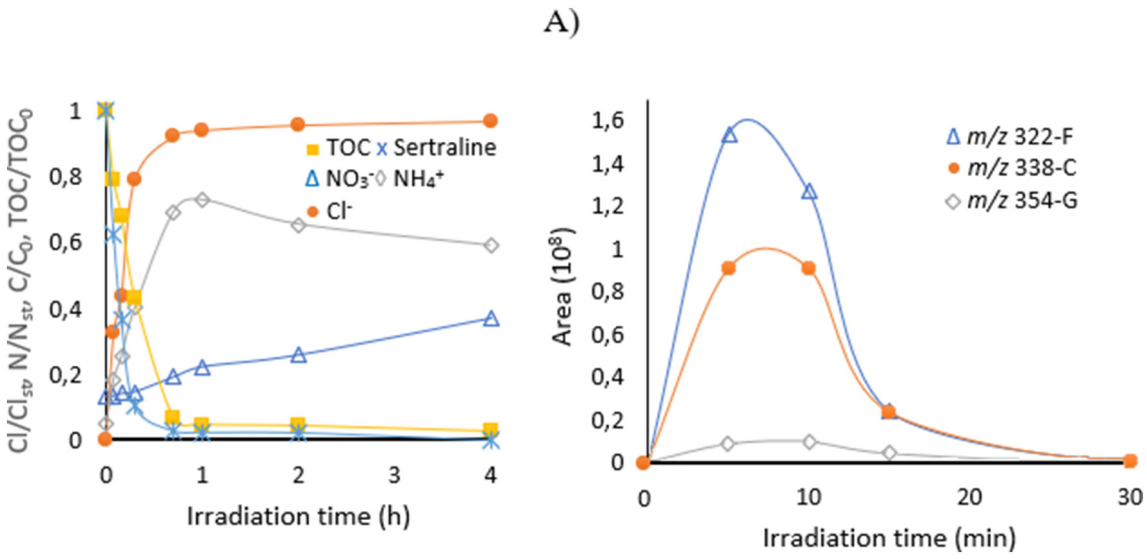

Fig. 2. Sertraline disappearance, TOC decrease and ammonium, nitrate, and chloride ions release (left) and some TPs (right) in the presence of TiO_2.

investigated by MS^n experiments, ascertaining the most likely losses from the protonated molecule ($[M + H]^+$ 306.0820). MS^2 spectrum presents the structural diagnostic ion at 275.0395 *m/z* that involves the detachment of methylamine from the tetrahydronaphthalene moiety (Table S2 and Fig. S1). MS^3 shows two peculiar fragments at 129.0697 *m/z*, due to the detachment of dichlorobenzene with the formation of the protonated dihydronaphtalene and 158.9756 *m/z*, resulting from the formation of the very stable dichlorotropylium cation, in agreement in literature data (Gornik et al., 2020).

Among the identified TPs, many of them are in the form of several isobaric species and their formation involves mono and polihydroxylation, oxidation, dehydration, dechlorination, cleavage of the molecule with the partial or total release of the dichlorophenyl moiety; their structural elucidation is presented below because of the reaction involved in their formation. All the identified TPs are collected in Fig, 4 and, based on the evolution profiles shown in Figs. S24 and S25, tentative transformation routes are proposed.

3.3.1. Hydroxylated compounds

We detected six species at *m/z* **322.0768**, five at *m/z* **338.0715** and ten at *m/z* **354.0661**, matched with formulae corresponding to the monohydroxy, dihydroxy and trihydroxysertraline, respectively. They are among the most abundant TPs, are quickly formed, reached the

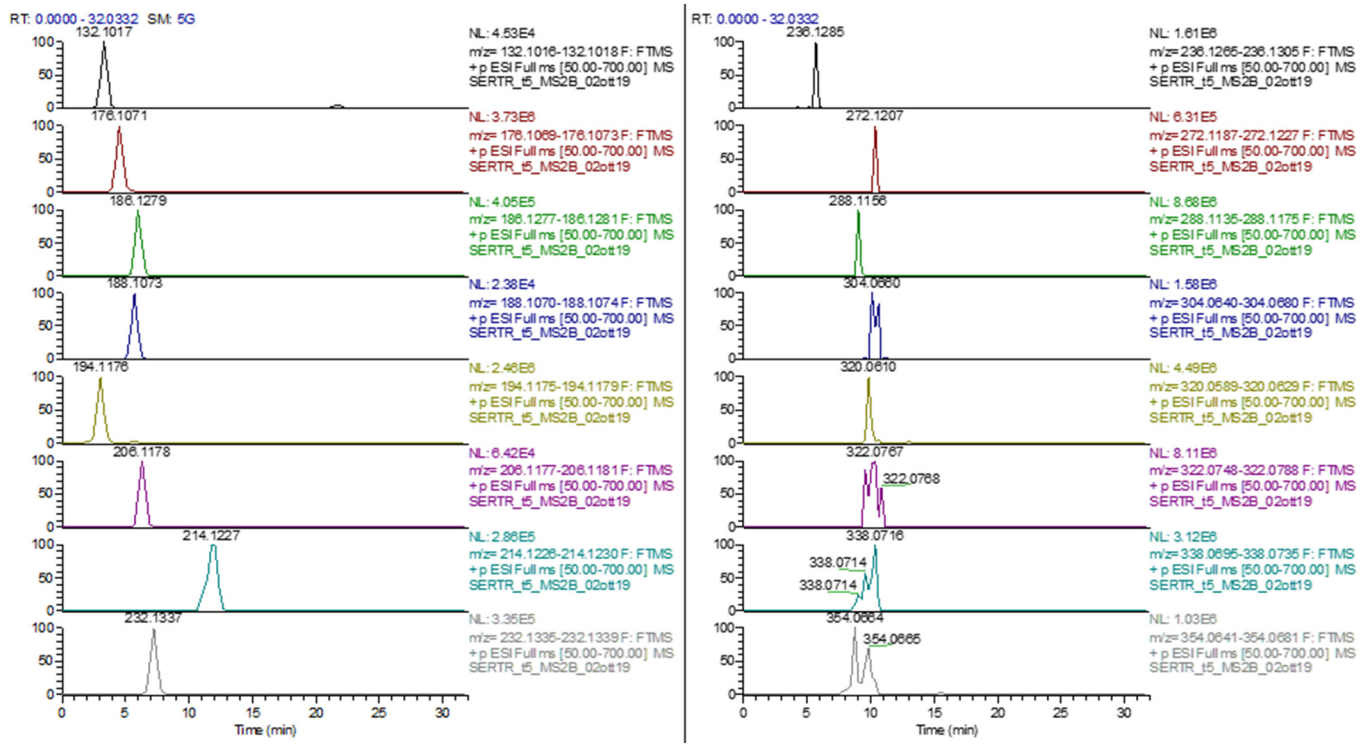

Fig. 3. LC-HRMS chromatogram showing main TPs formation at 5 min of photocatalytic degradation. On peaks top, *m/z* values are displayed.

Table 2
Sertraline and its transformation products formed during the photocatalytic process.

[M + H$^+$]	Empirical formula	Δmmu	DBE	RT (*min*)	Confidence level
306.0820 (sertraline)	$C_{17}H_{18}NCl_2$		9	13.10	L1
132.1017	$C_6H_{14}O_2N$	−0.205	1	2.89	L3
176.1071	$C_{11}H_{14}ON$	0.109	6	3.55	L2b
186.1279	$C_{13}H_{16}N$	0.174	7	5.59	L2b
188.1072	$C_{12}H_{14}ON$	0.209	7	13.58	L2b
194.1177	$C_{11}H_{16}O_2N$	0.145	5	2.89	L2b
206.1179	$C_{12}H_{16}O_2N$	0.345	6	5.97	L3
214.1228	$C_{14}H_{16}ON$	0.159	8	13.98	L3
232.1337	$C_{14}H_{18}O_2N$	0.495	7	7.42	L2b
236.1285	$C_{13}H_{18}O_3N$	0.380	6	5.14	L3
272.1207 (A, B)	$C_{17}H_{19}NCl$	0.646	9	12.20	L2b
288.1155 (A, B)	$C_{17}H_{19}ONCl$	0.532	9	10.34–10.84	L2b
304.0660	$C_{17}H_{16}NCl_2$	0.010	10	11.88	L2b
320.0609 (A, B)	$C_{17}H_{16}ONCl_2$	0.554	10	11.47	L2b, L2b
322.0768 (A, B, C, D, E, F)	$C_{17}H_{18}ONCl_2$	0.255	9	11.00 - 11.25 - 11.80- 12.03 - 12.44 - 12.99	L3-L3-L2b-L2b-L2b-L3
338.0715 (A, B, C, D, E)	$C_{17}H_{18}O_2NCl_2$	0,589	9	10.28 - 10.56 - 11.14- 11.68 - 12.39	L3-L3-L3-L2b-L3
352.0507	$C_{17}H_{16}O_3NCl_2$	0.525	10	11.79	L2
354.0661 (A, B, C, D, E, F, G, H, I, L)	$C_{17}H_{18}O_3NCl_2$	0,275	9	9.12 - 9.90 - 10.32- 10.50 - 10.89 - 11.19- 11.52 - 11.93 - 12.25 - 16.67	L3-L-L3-L3-L3-L3-L3-L3-L3-L2b

maxima amount after 5 min, and then completely disappear in 20 min of irradiation (see Fig. S24).

Monohydroxylation was already recognized to occur *via* biodegradation (Gornik et al., 2020) and photo-transformation (Jakimska A et al., n.d.) with the formation of two isomers, while we identified several bihydroxy and trihydroxysertraline isomers for the first time. The loss of unmodified methylamine was detected in their MS^2 spectra; therefore, a hydroxylation on the methylamine moiety can be excluded for all of them. No additional data useful to assign the OH position was available (see Tables S2–S4).

Analyzing monohydroxysertraline, isomers **C**, **D** and **E** share the fragment at *m/z* 129.0697 implying the detachment of the hydroxydichlorophenyl group; thus, based on their retention times, the three isomers bear the hydroxyl group on C2 (**E**), C5 (**C**) and C6 (**D**) of the phenyl ring (see Figs. S2 and S3-top). Conversely, isomers **A**, **B** and **F** display two product ions at *m/z* 145.0646 and 158.9756 in MS^3 spectrum, well-matched with the hydroxylation on the tetrahydronaphtyl moiety. Even if it was not possible to definitely elucidate their structures, for isomer **B** the loss of a molecule of water in MS^2 spectrum allows to place the OH group in the tetrahydro ring, while for isomers **A** and **F** hydroxylation occurs on the aromatic ring (see Fig. S3, bottom).

Considering dihydroxysertraline, **isomer B** bears both hydroxylations on the dichlorophenyl moiety as assessed by the formation of the ion at *m/z* 129.0697 in MS^3 spectrum, while **isomer A** produced the ions at *m/z* 145.0646 and 174.9712, consistent with one hydroxylation on the dichlorophenyl moiety and the other one on tetrahydronaphthalene.

Isomers C, **D** and **E** produce the ion at *m/z* 158.9756, coherent with the presence of both OH groups on the tetrahydronaphthalene unit; the formation of the complementary ion at *m/z* 161.0597 further supports this assumption (see Fig. S4). For **isomer D** the structural diagnostic loss of hydrogen peroxide (34.0062 Da) in MS^2 spectrum allows to locate the two OH groups on C2 and C3 (see Fig. S5). **Isomer E** bears the loss of a molecule of water MS^2 spectrum, thus signifying the presence of a hydroxy group in the tetrahydro ring. The fragment at *m/z* 158.9756 in MS^3 spectrum evidenced that the dichlorophenyl ring was not subjected to hydroxylation and, being the less polar isomer, we can tentatively postulate a hydroxylation on C2 prone to form a hydrogen bond with the amino group. In the case of isomer **C**, the absence of water losses suggests the presence of both OH groups on the aromatic moiety.

Regarding the trihydroxylated species, for isomer **L** the structural diagnostic ion at *m/z* 129.0697 permits to postulate that trihydroxylation took place on the free positions on the dichlorophenyl ring. For the other isobaric species, the available information is not enough for a definite structure elucidation but allows some considerations (see Fig. S6 and S7). The absence of water losses for isomers **A**–**D**, **F** and **G** permits to state that the hydroxylation occurring on tetrahydronaphthalene involved the aromatic portion. Additionally, for isomers **C**, **D** and **F** the ion at *m/z* 161.0597 is well-matched with the presence of two of the three OH groups on the dichlorophenyl moiety, while for isomers **A**, **B** and **G** the formation of the ion at 145.0646 *m/z* in MS^3 lets to place there only one OH group.

Conversely, isomers **E**, **H** and **I** hold the tri-hydroxylation on the tetrahydronaphthalene moiety as assessed by the formation of the ion at *m/z* 177.0546; the loss of a molecule of water in MS^2 spectrum advises that one of them is on the tetrahydro moiety and the other two on the aromatic portion.

Four TPs involved the formation of double bond(s) and are collected in Table S5 and Figs. S9–12. TP with [M + H]$^+$ **304.0660** and empirical formula $C_{17}H_{16}NCl_2$ is attributed to sertraline with a double bond; the loss of methylenamine (29.0266 Da) allows to place it on the methylamine moiety, in agreement with literature data (Jakimska A et al., n.d.).

Two TPs at *m/z* **320.0609** were detected and derived from one of the aforementioned monohydroxylated species. They practically coeluted and are distinguishable only by MS^n. Because of different fragmentation pathways these species are not the same of 320 *m/z* species identified by Gornik et al. (2020). **Isomer B** holds the double bond in the methylamine moiety, as assessed by the loss of methylenamine, and the hydroxyl group on the dichlorophenyl moiety, justified by the formation of the ions at *m/z* 129.0697 and 174.9712 in MS^3 spectrum; it reasonably comes from the reduction of 322 (C, D or E). Isomer **320 A** produces in MS^2 spectrum the neutral loss of 47.0372 Da attributed to methanolamine (see Fig. S11), reliable with the hydroxylation on the methylamine and a double bond formed in the tetrahydro ring.

TP at *m/z* **352.0507** was detected for the first time; it yields the double bond on the methylamine moiety owing to the loss of methylenamine. The formation of the ion at *m/z* 158.9756 allows locating the three hydroxyl groups on the tetrahydronaphthalene moiety; the loss of hydrogen peroxide in MS^3 spectrum (ions at *m/z* 289.0182) attested that the two OH groups are on C2 and C3 and the third one on the aromatic moiety (Fig. S12).

3.3.2. Dechlorinated compounds

We detected four de-chlorinated TPs quickly formed with a maximum evolution achieved in 5 min and a complete disappearance after 30 min of irradiation (see Fig. S24) collected in Table S6. Two of them involved a reductive dechlorination with the removal of one chlorine atom and the formation of two isobaric species at *m/z*

272.1207 (see Fig. S13), in agreement with literature data (Jakimska et al., n.d). We also detected two TPs at *m/z* **288.1155** formed through the replacement of a chlorine atom by an OH group. The formation of the cation chlorohydroxytropilium at *m/z* 141.0100 confirms the proposed structure (see Fig. S14).

3.3.3. Compounds at lower molecular weight

We identified nine TPs at lower molecular weight, whose formation involved the molecule breakage and occurred slower (maximum at 10 min of irradiation, see Fig. S24).

TPs with $[M + H]^+$ **176.1071** and **194.1177** are formed *via* the detachment of the dichlorophenyl ring followed by mono (or di)hydroxylation. TP at *m/z* 176 is one of the main TPs, already recognized *via* biotransformation (Gornik et al., 2020). Its MS^2 spectrum evidenced the loss of methylamine and of a molecule of water, suggesting a hydroxylation on the tetrahydro ring (see Table S7 and Fig. S15). TP at *m/z* 194.1177 was detected for the first time and, again, the loss of hydrogen peroxide with the formation of the fragment at *m/z* 160.1121 argues in favor of the two OH groups on C2 and C3 and to link its formation to the rupture of TP **338-D** (Fig. S16).

Finally, we detected for the first time six TPs at $[M + H]^+$ **186.1279**, **188.1072**, **236.1285**, **206.117**, **214.1228** and **232.1337** that involved a partial detachment of dichlorophenyl ring (see Tables S8–S10 for their MS^n ions). TPs 214 and 232 are abundant and easily formed, while TPs 186, 188, 236 and 206 are among the less abundant by-products and their formation is delayed.

TPs with $[M + H]^+$ **236.1285** and **206.1179** and empirical formulae $C_{13}H_{18}O_3N$ and $C_{12}H_{16}O_2N$ hold a carboxylic group. The former exhibits the loss of two molecules of water (fragments at *m/z* 218.1179 and 200.1073), the joint losses of water and methylamine (*m/z* 187.0756)

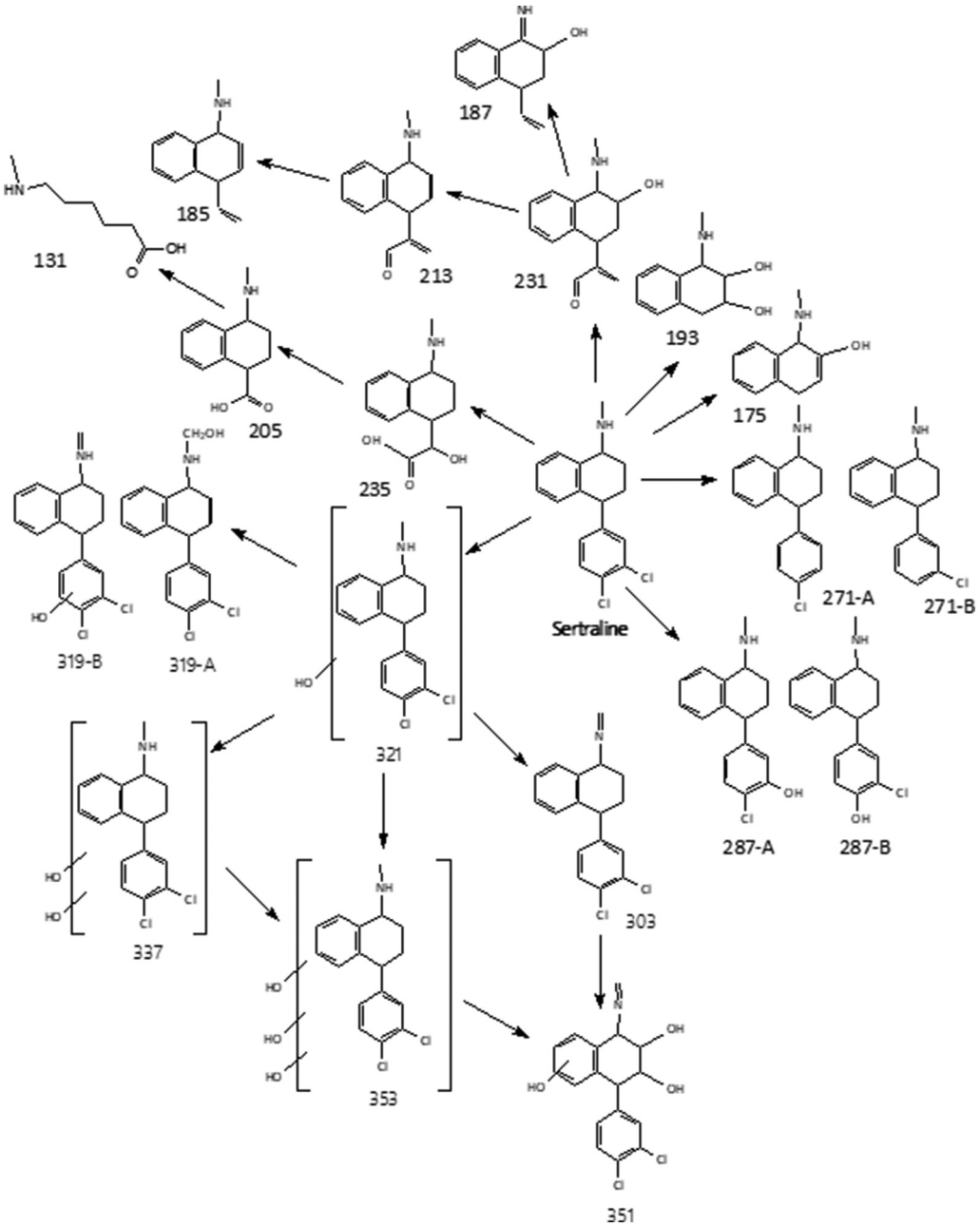

Fig. 4. Main transformation products formed during the photocatalytic process.

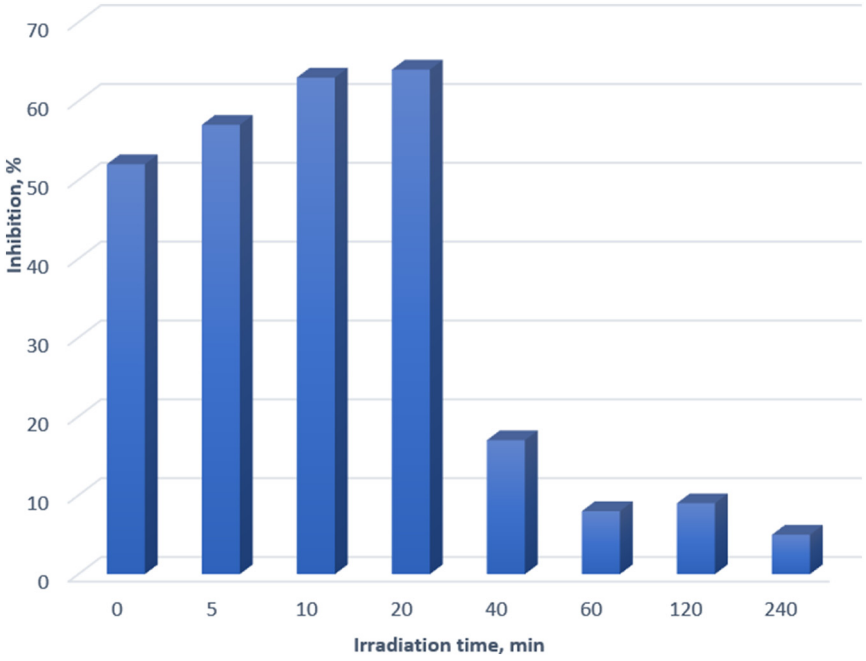

Fig. 5. Toxicity assessed for sertraline as a function of the irradiation times.

and of methylamine and formic acid (*m/z* 159.0804) (Fig. S17), while the latter involved the loss of methylamine (ion at *m/z* 175.0755) and formic acid as well (*m/z* 129.0697) (Fig. S18).

The species with $[M + H]^+$ **214.1228** and **232.1337** result from a partially oxidized chain. The proposed structures are shown in Figs. S19–20 and are justified by the joint loss of CO and methylamine, with the formation of the ion at *m/z* 155.0855. The absence of other losses could be the result of the highly stable ion formed. Furthermore, for TP at *m/z* 232.1337 the loss of a molecule of water is consistent with the hydroxylation on the tetrahydro ring.

A species at $[M + H]^+$ **188.1072** is formed from TP 232 through a demethylation and the detachment of CO. It forms the fragment at *m/z* 160.0757 *via* the loss of a molecule of ethylene and at *m/z* 131.0583 through the ring opening *via* the loss of C_2H_3NO and ethylene (see Fig. S21). Considering *m/z* 186.1279, it comes from TP 214 *via* CO loss. MS^2 spectrum shows the loss of ethylene (ion at *m/z* 158.0695), so we can postulate the structure shown in Fig. 4.

Lastly, TP at *m/z* **132.1017** exhibits a linear structure, is one of the most abundant TPs and its formation is delayed, as assessed in Fig. S25. MS^2 spectrum forms the ion at *m/z* 86.0960 through the loss of formic acid, well matched with the proposed structure (see Figs. 4 and S23).

3.4. Toxicity of sertraline and its TPs

The potential acute toxicity of sertraline and its formed TPs was assessed *via* the *Vibrio fischeri* bioassays by assessing the inhibition on the luminescent bacteria emission. The samples resulting from the photocatalytic degradation as a function of irradiation time are plotted (Fig. 5). Sertraline is a moderately toxic compound (EC_{50} = 20 mg/L) and its transformation in the first steps proceeded through the formation of toxic compounds. The percentage of inhibition increased up to 70%, at irradiation times when the larger part of TPs was formed. Then after 20 min of irradiation, the toxicity of the irradiated solution decreased to levels

Table 3
Toxicity predictions for sertraline (SER) and its transformation products using ECOSAR software.

$[M + H^+]$	Empirical formula	Acute toxicity [mg/L]			Chronic toxicity (ChV) [mg/L]		
		Fish (LC_{50})	Daphid (LC_{50})	Algae (EC_{50})	Fish	Daphid	Algae
306.0820 (SERT)	$C_{17}H_{18}NCl_2$	0.408	0.071	0.028	0.0074	0.0085	0.012
132.1017	$C_6H_{14}O_2N$	1.02×10^3	91.8	133	142	5.71	35.9
176.1071	$C_{11}H_{14}ON$	126	13.6	13.7	10.0	1.01	4.24
186.1279	$C_{13}H_{16}N$	3.33	0.476	0.274	0.111	0.047	0.104
188.1072	$C_{12}H_{14}ON$	5.96	3.92	5.31	0.692	0.572	1.92
194.1177	$C_{11}H_{16}O_2N$	558	54.0	67.0	61.3	3.62	19.2
206.1179	$C_{12}H_{16}O_2N$	7.94×10^4	6.29×10^3	1.16×10^4	1.60×10^4	348	2.88×10^3
214.1228	$C_{14}H_{16}ON$	19.4	2.45	1.80	0.949	0.213	0.624
232.1337	$C_{14}H_{18}O_2N$	156	16.9	16.8	12.2	1.26	5.22
236.1285	$C_{13}H_{18}O_3N$	1.59×10^5	1.21×10^4	2.43×10^4	3.66×10^4	641	5.84×10^3
272.1207 (A, B)	$C_{17}H_{19}NCl$	0.960	0.156	0.070	0.022	0.017	0.029
288.1155 (A, B)	$C_{17}H_{19}ONCl$	2.10	0.322	0.162	0.057	0.034	0.064
304.0660	$C_{17}H_{16}NCl_2$	0.078	0.132	0.00072	0.0018	0.021	0.019
320.0609 (A, B)	$C_{17}H_{16}ONCl_2$	0.053	0.155	0.0054	0.0080	0.036	0.032
322.0768 (A, B, C, D, E, F)	$C_{17}H_{18}ONCl_2$	0.887	0.147	0.063	0.019	0.017	0.027
338.0715 (A, B, C, D, E)	$C_{17}H_{18}O_2NCl_2$	1.93	0.301	0.154	0.049	0.032	0.059
352.0507	$C_{17}H_{16}O_3NCl_2$	3.96	3.50	0.371	0.461	0.504	1.14
354.0661 (A, B, C, D, E, F, G, H, I, L)	$C_{17}H_{18}O_3NCl_2$	4.17	0.616	0.332	0.126	0.062	0.129

around 10%. The samples from 40 min present a significantly lower inhibition in agreement with the complete removal of the observed identified TPs and the significant mineralization observed, as shown in Fig. 5. Since the identified TPs of SER are not commercially available, ECOSAR program was employed as a good alternative to derive toxicity data for fish, daphnia, and algae and to link the toxicity results obtained by luminescent bacterium test. This program can screen and predict the aquatic toxicity of chemicals based on the similarity of structure to chemicals for which the aquatic toxicity has been previously reported, and therefore is widely used to predict acute and chronic toxicity of compounds observed during water treatment processes (Kuang et al., 2013). Data at Table 3 show that the LC_{50} obtained for SER for fish was about 0.408 mg/L, whilst LC_{50} and EC_{50} were much lower for daphnid and green algae (about 0.071 and 0.028 mg/L respectively). Considering the ranking of these toxicity values, almost all the TPs produced during the photocatalytic treatment of SERT exhibited higher toxicity than the parent molecule in contrast to photolytic experiments where the ECOSAR toxicity prediction software showed that transformation products will either have comparable or lower toxicity than their parent compound (Gornik et al., 2019). Special attention (Table 3) should be given to TPs $m/z = 236.1285$, $m/z = 206.1179$ and $m/z = 132.1017$ that exhibit based on the ECOSAR program LC_{50} for fish up to 1.59×10^5 mg/L. Probably, the employment of multi-species is crucial for evaluating the toxicity during such treatments. Nevertheless, it should be also noted that other TPs, which were not identified under the given experimental conditions, might also contribute to the increased toxicity in the early stages of the photocatalytic treatment.

4. Conclusions

The photolytic and photocatalytic behavior of antidepressant drug sertraline was investigated under simulated solar irradiation. Results have shown that first-order kinetics were followed, and that indirect photolysis demonstrate a significant contribution to the environmental fate of sertraline in aquatic systems. Introduction of titania as a catalyst dramatically accelerated the process even at mild conditions (400 mg/L) and after 1 h of irradiation, both parent molecule and its TPs were totally removed. Forty-four transformation products were identified by means of high-resolution mass spectrometry, seventeen of them are reported for the first time. Our findings demonstrate that identification of transformation byproducts although a very challenging analytical process could bring some substantial knowledge with regards to the "targeted" determination of potential transformation products in environmental aquatic systems considering the fact that thirty four of these chemicals display higher acute toxicity potential (based on ECOSAR software).

CRediT authorship contribution statement

Paola Calza: Conceptualization, Resources, Writing - original draft, Writing - review & editing. **Cristina Jiménez-Holgado:** Methodology, Validation, Formal analysis, Investigation, Visualization, Writing - original draft. **Marco Coha:** Investigation. **Christoforos Chrimatopoulos:** Methodology, Validation, Formal analysis, Investigation, Visualization, Writing - original draft. **Federica Dal Bello:** Investigation. **Claudio Medana:** Methodology, Formal analysis. **Vasilios Sakkas:** Conceptualization, Methodology, Resources, Writing - original draft, Writing - review & editing, Visualization.

Declaration of competing interest

The authors declare no conflicts of interest.

Acknowledgements

This work is part of a project that has received funding from the European Union's Horizon 2020 research and innovation programme under the Marie Skłodowska-Curie Grant Agreement No 765860 (AQUAlity).

Appendix A. Supplementary data

Supplementary data to this article can be found online at https://doi.org/10.1016/j.scitotenv.2020.143805.

References

Baker, D.R., Kasprzyk-Hordern, B., 2011. Multi-residue analysis of drugs of abuse in wastewater and surface water by solid-phase extraction and liquid chromatography-positive electrospray ionisation tandem mass spectrometry. J. Chromatogr. A 1218 (12), 1620–1631. https://doi.org/10.1016/j.chroma.2011.01.060.

Calza, P., Sakkas, V.A., Medana, C., et al., 2006. Photocatalytic degradation study of diclofenac over aqueous TiO2 suspensions. Appl. Catal. B Environ. 67 (3–4), 197–205. https://doi.org/10.1016/j.apcatb.2006.04.021.

El Mouchtari, E.M., Daou, C., Rafqah, S., et al., 2020. TiO2 and activated carbon of Argania Spinosa tree nutshells composites for the adsorption photocatalysis removal of pharmaceuticals from aqueous solution. J. Photochem. Photobiol. A Chem. 388 (October), 112183. https://doi.org/10.1016/j.jphotochem.2019.112183.

Gornik, T., Vozic, A., Heath, E., Trontelj, J., Roskar, R., Zigon, D., Vione, D., Kosjek, T., 2019. Determination and photodegradation of sertraline residues in aqueous environment. Environ. Pollut. 256, 113431. https://doi.org/10.1016/j.envpol.2019.113431.

Gornik, T., Kovacic, A., Heath, E., Hollender, J., Kosjek, T., 2020. Biotransformation study of antidepressant sertraline and its removal during biological wastewater treatment. Water Res. 181, 115864. https://doi.org/10.1016/j.watres.2020.115864.

Hernando, M.D., Mezcua, M., Fernández-Alba, A.R., Barceló, D., 2006. Environmental risk assessment of pharmaceutical residues in wastewater effluents, surface waters and sediments. Talanta 69 (2 SPEC. ISS), 334–342. https://doi.org/10.1016/j.talanta.2005.09.037.

Hörsing, M., Kosjek, T., Andersen, H.R., Heath, E., Ledin, A., 2012. Fate of citalopram during water treatment with O3, ClO2, UV and Fenton oxidation. Chemosphere 89 (2), 129–135. https://doi.org/10.1016/j.chemosphere.2012.05.024.

A. Jakimska, M. Śliwka Kaszyńska, P. Nagórski, A. Kot Wasik and J. Namieśnik, Environmental fate of two psychiatric drugs, diazepam and sertraline: phototransformation and investigation of their photoproducts in natural waters. J. Chromatogr. Sep. Tech. 5: 253, https://doi.org/10.4172/2157-7064.1000253.

Kang, Y.M., Kim, M.K., Zoh, K.D., 2018. Effect of nitrate, carbonate/bicarbonate, humic acid, and H2O2 on the kinetics and degradation mechanism of Bisphenol-A during UV photolysis. Chemosphere 204, 148–155. https://doi.org/10.1016/j.chemosphere.2018.04.015.

Katagi, T., 2018. Direct photolysis mechanism of pesticides in water. J. Pestic. Sci. 43 (2), 57–72. https://doi.org/10.1584/jpestics.D17-081.

Klavarioti, M., Mantzavinos, D., Kassinos, D., 2009. Removal of residual pharmaceuticals from aqueous systems by advanced oxidation processes. Environ. Int. 35 (2), 402–417. https://doi.org/10.1016/j.envint.2008.07.009.

Kosjek, T., Heath, E., 2008. Applications of mass spectrometry to identifying pharmaceutical transformation products in water treatment. TrAC Trends Anal. Chem. 27 (10), 807–820. https://doi.org/10.1016/j.trac.2008.08.014.

Kosjek, T., Heath, E., 2010. Tools for evaluating selective serotonin re-uptake inhibitor residues as environmental contaminants. TrAC Trends Anal. Chem. 29 (8), 832–847. https://doi.org/10.1016/j.trac.2010.04.012.

Kosjek, T., Heath, E., Krbavčič, A., 2005. Determination of non-steroidal anti-inflammatory drug (NSAIDs) residues in water samples. Environ. Int. 31 (5), 679–685. https://doi.org/10.1016/j.envint.2004.12.001.

Kuang, J., Huang, J., Wang, B., Cao, Q., Deng, S., Yu, G., 2013. Ozonation of trimethoprim in aqueous solution: identification of reaction products and their toxicity. Water Res. 47 (8), 2863–2872. https://doi.org/10.1016/j.watres.2013.02.048.

Lajeunesse, A., Smyth, S.A., Barclay, K., Sauvé, S., Gagnon, C., 2012. Distribution of antidepressant residues in wastewater and biosolids following different treatment processes by municipal wastewater treatment plants in Canada. Water Res. 46 (17), 5600–5612. https://doi.org/10.1016/j.watres.2012.07.042.

Minero, C., Pelizzetti, E., Sega, M., Friberg, S.E., Sjöblom, J., 1999. The role of humic substances in the photocatalytic degradation of water contaminants. J. Dispers. Sci. Technol. 20 (1–2), 643–661. https://doi.org/10.1080/01932699908943812.

Mole, R.A., Brooks, B.W., 2019. Global scanning of selective serotonin reuptake inhibitors: occurrence, wastewater treatment and hazards in aquatic systems. Environ. Pollut. 250, 1019–1031. https://doi.org/10.1016/j.envpol.2019.04.118.

Nassar, R., Trivella, A., Mokh, S., Al-Iskandarani, M., Budzinski, H., Mazellier, P., 2017. Photodegradation of sulfamethazine, sulfamethoxypiridazine, amitriptyline, and clomipramine drugs in aqueous media. J. Photochem. Photobiol. A Chem. 336, 176–182. https://doi.org/10.1016/j.jphotochem.2016.12.008.

Niu, J., Li, Y., Wang, W., 2013. Light-source-dependent role of nitrate and humic acid in tetracycline photolysis: kinetics and mechanism. Chemosphere 92 (11), 1423–1429. https://doi.org/10.1016/j.chemosphere.2013.03.049.

Ofoegbu, P.U., Lourenço, J., Mendo, S., Soares, A.M.V.M., Pestana, J.L.T., 2019. Effects of low concentrations of psychiatric drugs (carbamazepine and fluoxetine) on the freshwater planarian, Schmidtea mediterranea. Chemosphere 217, 542–549. https://doi.org/10.1016/j.chemosphere.2018.10.198.

Pozdnyakov, I.P., Tyutereva, Y.E., Parkhats, M.V., et al., 2020. Mechanistic investigation of humic substances assisted photodegradation of imipramine under

simulated sunlight. Sci. Total Environ. 738, 140298. https://doi.org/10.1016/j.scitotenv.2020.140298.
Schymanski, E.L., Jeon, J., Gulde, R., et al., 2014. Identifying small molecules via high resolution mass spectrometry: communicating confidence. Environ. Sci. Technol. 48 (4), 2097–2098. https://doi.org/10.1021/es5002105.
Sugihara, M.N., Moeller, D., Paul, T., Strathmann, T.J., 2013. TiO2-photocatalyzed transformation of the recalcitrant X-ray contrast agent diatrizoate. Appl. Catal. B Environ. 129, 114–122. https://doi.org/10.1016/j.apcatb.2012.09.013.
Talwar, S., Sangal, V.K., Verma, A., 2018. Feasibility of using combined TiO2 photocatalysis and RBC process for the treatment of real pharmaceutical wastewater. J. Photochem. Photobiol. A Chem. 353, 263–270. https://doi.org/10.1016/j.jphotochem.2017.11.013.
Tay, K.S., Madehi, N., 2015. Ozonation of ofloxacin in water: by-products, degradation pathway and ecotoxicity assessment. Sci. Total Environ. 520, 23–31. https://doi.org/10.1016/j.scitotenv.2015.03.033.
Trawiński, J., Skibiński, R., 2017. Studies on photodegradation process of psychotropic drugs: a review. Environ. Sci. Pollut. Res. Int. 24 (2), 1152–1199. https://doi.org/10.1007/s11356-016-7727-5.
Trawiński, J., Skibiński, R., 2019. Rapid degradation of clozapine by heterogeneous photocatalysis. Comparison with direct photolysis, kinetics, identification of transformation products and scavenger study. Sci. Total Environ. 665, 557–567. https://doi.org/10.1016/j.scitotenv.2019.02.124.
Vione, D., Minella, M., Maurino, V., Minero, C., 2014. Indirect photochemistry in sunlit surface waters: Photoinduced production of reactive transient species. Chem. Eur. J. 20 (34), 10590–10606. https://doi.org/10.1002/chem.201400413.
Wu, M., Xiang, J., Que, C., Chen, F., Xu, G., 2015. Occurrence and fate of psychiatric pharmaceuticals in the urban water system of Shanghai, China. Chemosphere 138, 486–493. https://doi.org/10.1016/j.chemosphere.2015.07.002.
Xiang, J., Wu, M., Lei, J., Fu, C., Gu, J., Xu, G., 2018. The fate and risk assessment of psychiatric pharmaceuticals from psychiatric hospital effluent. Ecotoxicol. Environ. Saf. 150 (December 2017), 289–296. https://doi.org/10.1016/j.ecoenv.2017.12.049.
Xie, Z., Lu, G., 2019. Interactive effects of sertraline and diphenhydramine on biochemical and behavioral responses in crucian carp (Carassius auratus). Int. J. Environ. Res. Public Health 16 (17). https://doi.org/10.3390/ijerph16173137.
Zhu, M., Ma, L., Zhang, D., Ray, K., Zhao, W., Humphreys, W.-G., Skiles, G., Sanders, M., Zhang, H., 2006. Detection and characterization of metabolites in biological matrices using mass defect filtering of liquid chromatography/high resolution mass spectrometry data. Drug Metab. Dispos. 34 (10), 1722–1733. https://doi.org/10.1124/dmd.106.009241.